NINETEENTH EUROPEAN ROTORCRAFT FORUM

Paper n° O7

DETECTION AND IDENTIFICATION OF THE NONLINEARITIES PRESENT ON A HELICOPTER FROM A FREQUENCY RESPONSE FUNCTION SET.

by

L. Luti and S. Speziali

AGUSTA, ITALY

September 14-16, 1993
CERNOBBIO (Como)
ITALY

ASSOCIAZIONE INDUSTRIE AEROSPAZIALI
ASSOCIAZIONE ITALIANA DI AERONAUTICA ED ASTRONAUTICA

DETECTION AND IDENTIFICATION OF THE NONLINEARITIES PRESENT ON A HELICOPTER FROM A FRF SET.

Luigi Luti and Saverio Speziali
Sistema Dinamico - AGUSTA

ABSTRACT

The nonlinearities present in a helicopter resting on ground were detected and identified from a experimental Frequency Response Function set.

In order to assure that only the nonlinearities belonging to helicopter structure were measured, a particular attention was devoted to the experiment set-up.

The Frequency Response Function set was obtained by the use of the stepped sine excitation technique with a closed control loop in both amplitude and frequency.

The analysis was performed by use of the Complex Stiffness Method, a Single Degree Of Freedom frequency domain technique. It allows not only to detect the existence of any nonlinear stiffness or damping but also to identify the type of nonlinearity. In this paper, after a brief theorethical introduction to the method, the obtained nonlinear damping and stiffness characteristics are presented and discussed.

1. INTRODUCTION

In the context of a methodological research programme, a series of ground measurements were performed on an Agusta helicopter airframe.

The comparisons of the Frequency Response Functions (FRFs), obtained at the same points for increasing excitation force level, showed important discrepancies: the natural frequency shifts to a lower level and the peak amplitude decreases. These observed phenomena, together with the unsymmetrical shape of the peaks, clearly indicate the presence of some form of nonlinear behaviour. The frequency response functions obtained at the driving point for four increasing lateral forces are shown in **Fig. 1**. A softening nonlinear behaviour is evident in both the first and second mode.

Modal analysis investigations are usually performed on the basis of the assumption of structural system linearity. When the system does not satisfy this fundamental assumption, completely erroneous modal model can result.

Therefore, if the existence of some nonlinearities is detected, it will be necessary to decide between two alternatives. Either, according to the common practice, to be satisfied with its detection and, by use of particular acquisition techniques (*e.g.*, random excitation), to reduce their consequence and relegate their residual effect to experimental error or to adopt a fully nonlinear approach in order to identify and quantify their characteristics.

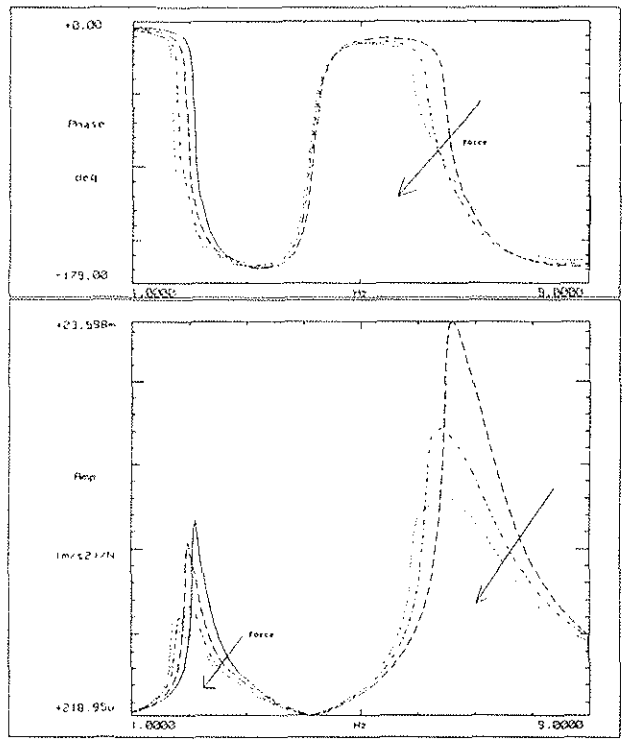

Fig. 1 - Measured frequency response function for increasing force excitation levels. 150, 300, 525, 750 *N*.

As the model identification results had to be used for a following verification procedure and the nonlinear behaviour was significant, the last alternative was preferred.

Because the two identifiable modes were quite uncoupled and separated from each other, it was reasonable to assume, obviously in a limited frequency range around them, the system behaves as a Single Degree Of Freedom system. This approach, neglecting the influence of the other modes, allowed the use of a SDOF identification and characterization method.

The Complex Stiffness Method **[1-4]** was chosen because of its possibility to be directly applied, under appropriate conditions, to the frequency response functions, *i.e.* the result of every general modal experimental testing, without requiring further dedicated measurements. Moreover, it does not need any a priori information or initial estimates of the nonlinear characteristics and it gives a physical insight in the nonlinear phenomena. The basis of the method is the describing function theory, proposed for the first time by Kochenburger in 1950 and usually applied in the control system theory **[5-8]**.

2. EXPERIMENTAL SET-UP

A frequency response function set was obtained by using the stepped sine excitation technique **[9]**. It is quite a new method that was developed for the analysis of both nonlinear and complex systems. This excitation method involves an incremental, stationary, sinusoidal excitation. A fully sinusoidal input is applied to the structure and the data are acquired only after the system has reached steady state conditions at the actual excitation frequency. The sinusoidal excitation frequency is varied in discrete step and the excitation amplitude is kept at constant level by a closed loop control. From the acquired time histories only the fundamental signal component is retained for the FRF calculation. By means of a repeated execution of this procedure for all spectral lines, input/output relations are accumulated as a function of the frequency.

The excitation was provided in both lateral and fore/aft directions. The shaker was connected to the helicopter so that the force could act perpendicularly to the rotor hub and could pass through the rotor disc centre. Indeed one of the essential conditions for proper use of the stepped sine technique is a absolutely unidirectional excitation.

Furthermore in order to single out the possible nonlinear effects, due to the structure/shaker interface, three different links between the shaker and the structure were used:

1) a spherical bearing; characterised by a non negligible backlash, but providing the transmission of high force level without introducing any significant misalignment;
2) a universal joint, characterised by a smaller backlash at low force level;
3) a stinger, a stiff connection without any backlash, but recovering only very small misalignment.

Several airborne configurations were taken into account to extract the effects of the position of the landing-gear shock struts. In order to insulate the structure from the support frame, the aircraft was suspended from the centre of the rotor hub by a pneumatic suspension. Such a way led to a variability of the suspension system: in the four airborne configurations the weight of the helicopter carried by the suspension ranged from 0 to 75 % of the aircraft global weight. Despite this change in weight, the rigid body eigenfrequencies had to be maintained below .8 *Hz*. This requirement was accomplished by adjusting the pressure in the pneumatic spring, maintaining constant the vertical height.

3. THEORETICAL ASPECTS

The dynamic behaviour of a nonlinear SDOF system can be described by the following equation:

$$m(\ddot{x},\dot{x},x)\ddot{x} + c(\ddot{x},\dot{x},x)\dot{x} + k(\ddot{x},\dot{x},x)x = f$$

where $m(\ddot{x},\dot{x},x)$, $c(\ddot{x},\dot{x},x)$ and $k(\ddot{x},\dot{x},x)$ are general nonlinear relationships.

When using stepped sine testing technique the FRFs are acquired frequency by frequency, limiting the spectral content of the output response at a pure sinusoidal input to its principal component. Such procedure is equivalent to applying the describing function linearization technique to the nonlinear input/output relationship.

In fact the describing function of a nonlinear system is defined to be the complex ratio of the fundamental component of the output to the pure sinusoidal input.

For a sinusoidal input $y(t) = Y\sin(\omega t)$ the output $w(t)$ of a general system will be a nonsinusoidal periodic function which can be expressed as a Fourier series as it follows:

$$w(t) = \sum_{n=0}^{\infty}\left(A_n\sin(n\omega t) + B_n\cos(n\omega t)\right) =$$

$$= A_0 + \sum_{n=1}^{\infty} W_n\sin(n\omega t + \varphi)$$

where:

$$A_n = \frac{1}{\pi}\int_0^{2\pi} w(t)\sin(n\omega t)d(\omega t)\ ;$$

$$B_n = \frac{1}{\pi}\int_0^{2\pi} w(t)\cos(n\omega t)d(\omega t)\,;$$

$$W_n = \sqrt{A_n^2 + B_n^2}\;;\quad \varphi_n = \tan^{-1}\left(\frac{B_n}{A_n}\right)$$

If the nonlinear relation between the input and the output of the element is symmetrical about the origin, then $A_0 = 0$. The fundamental component of the output is:

$$w_1(t) = A_1\sin(\omega t) + B_1\cos(\omega t) = W_1\sin(\omega t + \varphi)$$

According to the previous definition the describing function is given by:

$$N(Y,\omega) = \frac{W_1}{Y}\angle\varphi_1 = \frac{A_1}{Y} + j\frac{B_1}{Y}$$

Generally the describing functions depends on the frequency and amplitude of the input signal. There are, however, a number of special cases.

If the force $f(t)$ is considered as the output and the displacement $x(t)$ as the pure sinusoidal input, the fundamental coefficients of the force Fourier series will result:

$$A_1 = \frac{X}{\pi}\left\{\int_0^{2\pi}\left[k(\ddot{x},\dot{x},x)x + m(\ddot{x},\dot{x},x)\ddot{x}\right]\sin(\omega t)d(\omega t) + \right.$$

$$\left. + \int_0^{2\pi} c(\ddot{x},\dot{x},x)\dot{x}\sin(\omega t)d(\omega t)\right\}$$

$$B_1 = \frac{X}{\pi}\left\{\int_0^{2\pi}\left[k(\ddot{x},\dot{x},x)x + m(\ddot{x},\dot{x},x)\ddot{x}\right]\cos(\omega t)d(\omega t) + \right.$$

$$\left. + \int_0^{2\pi} c(\ddot{x},\dot{x},x)\dot{x}\cos(\omega t)d(\omega t)\right\}$$

Considering the describing function definition, after straightforward calculations:

$$\frac{A_1}{X} = N_o^k(X,\omega) - \omega^2 N_o^m(X,\omega) + \omega N_e^c(X,\omega)$$

$$\frac{B_1}{X} = N_e^k(X,\omega) - \omega^2 N_e^m(X,\omega) + \omega N_o^c(X,\omega)$$

where the subscript o and e indicates respectively the describing function of the odd and the even part (or, in a more general sense, its real and imaginary parts) of the $m(\ddot{x},\dot{x},x)$, $c(\ddot{x},\dot{x},x)$ and $k(\ddot{x},\dot{x},x)$ relationships, and the superscripts indicate the parameter described by the considered describing function (m for mass, c for damping and k for stiffness).

3.1 Complex Stiffness Method

If the following simplifying hypotheses are assumed:

1) the mass $m(\ddot{x},\dot{x},x) = \overline{m}$ = constant;
2) the stiffness $k(\ddot{x},\dot{x},x) = k(x)$ is an odd function of the only displacement;
3) the damping $c(\ddot{x},\dot{x},x) = c(\dot{x})$ is an odd function of the only velocity;

the describing function of the whole system under those conditions will become:

$$N^s(X) = \frac{A_1}{Y} + j\frac{B_1}{Y} = \left[N_o^k(X,\omega) - \omega^2\overline{m}\right] + j\left[\omega N_o^c(X,\omega)\right]$$

Comparing the previous expression with the inverse of the compliance of a single degree of freedom:

$$\frac{F}{X} = \left(k_{eq} - \omega^2 m_{eq}\right) + j\left(\omega c_{eq}\right)$$

their similarity is evident.

Because the describing function of the dynamic relationship was calculated with the force as output and the displacement as input, while the actual (experimental like) FRF is obtained with the displacement as output and the force as input, it is clear that m_{eq}, k_{eq} and c_{eq} will coincide with the $\overline{m}$, $N_o^k(X,\omega)$ and $N_o^c(X,\omega)$ only if the harmonics of the actual output are negligible in comparison with its fundamental component. In fact the inverse of a describing function is not necessary identical to the describing function of the inverse.

In the experimental testing the inertance is usually acquired:

$$\frac{F}{\ddot{X}} = \left(\overline{m} - \frac{k_{eq}}{\omega^2}\right) - j\left(\frac{c_{eq}}{\omega}\right) = \Re e\left(\frac{F}{\ddot{X}}\right) + j\,\Im m\left(\frac{F}{\ddot{X}}\right)$$

In the previous expressions it is easily noticed one of the most intriguing aspects of the Complex Stiffness Method: while the direct FRF of a SDOF system tends to mix together the stiffness and mass characteristics with the damping ones, the inverse FRF separates them respectively in the real and imaginary part.

The system parameters are related to the real and imaginary parts of the inverse inertance according to the following expressions:

$$k_{eq} = \left[\overline{m} - \Re e\left(\frac{F}{\ddot{X}}\right)\right]\omega^2$$

$$c_{eq} = -\omega\,\Im m\left(\frac{F}{\ddot{X}}\right)$$

It is clear that, providing the mass is known, k_{eq} and c_{eq} can be calculated as a function of the frequency and consequently also as functions of displacement and velocity.

3.2 Mass Calculation

Taking into account two points of the FRF with identical displacement magnitude, it is possible to write the following expressions:

$$\text{Point 1:} \quad R_1 = \Re e_1\left(\frac{F}{\ddot{X}}\right) = \overline{m} - \frac{k_1}{\omega_1^2}$$

$$\text{Point 2:} \quad R_2 = \Re e_2\left(\frac{F}{\ddot{X}}\right) = \overline{m} - \frac{k_2}{\omega_2^2}$$

since the stiffness was assumed to be function of the only displacement its values will be identical for both the points. This allows the elimination of k_1 and k_2 values from the two expressions and yields to the following relation:

$$\overline{m} = \left[R_1 - \left(\frac{\omega_2}{\omega_1}\right)^2 R_2\right]\left(\frac{\omega_1^2}{\omega_1^2 - \omega_2^2}\right)$$

If this procedure is repeated for each couple of points corresponding to a certain displacement, a relating value of the mass can be estimated. Then the mass values could be averaged over the whole frequency range.

An alternative technique is available in the case where the previous method failed (*e.g.*, when jump phenomena are present in the FRFs or when the stiffness is also dependent on velocity or frequency). After collecting different values at the same frequency but obtained with different force magnitudes, the curve $\left(k_{eq} - \omega^2 m\right)$ is set as a function of displacement. Next, it is possible to extrapolate its value for $x = 0$. The whole procedure is repeated for at least another frequency. Assuming that for all the frequencies the stiffness values, obtained for $x = 0$, are constant, the mass can be estimated from the curve $\left(k_{eq}^{|x=0|} - \omega^2 m\right)$.

3.3 Parameters Actual Values

As just said the m_{eq}, c_{eq} and k_{eq} are the describing functions of the actual parameters. Generally, in order to describe the dynamic behaviour with a more accurate nonlinear model, instead of the linearized describing function representation, the reconstruction of the original nonlinear characteristics could be an interesting goal.

It can be shown [see appendix **A1** for the demonstration of a common simple example], that the describing function for an odd piecewise linear nonlinearity can be written in the form

$$N(X) = \sum_{i=1}^{n-1}(k_i - k_{i+1})S\left(\frac{\delta_i}{X}\right) + k_n$$

where:

n is the number of the linear segments;

δ_i is the ith breakpoint;

k_i is the slope of the input/output linear relationship occurring for $\delta_{i-1} \le x \le \delta_i$;

and $S(\delta/X)$ is called the saturation function and it is defined as:

$$S\left(\frac{\delta_i}{X}\right) = \begin{cases} \frac{2}{\pi}\sin^{-1}\left(\frac{\delta}{X}\right) + \frac{\delta}{X}\sqrt{1 - \left(\frac{\delta}{X}\right)^2} & \text{for } \left(\frac{\delta}{X}\right) \le 1 \\ 1 & \text{for } \left(\frac{\delta}{X}\right) > 1 \end{cases}$$

Computing $N(X)$ for $X = \frac{\delta_0 + \delta_1}{2}, \frac{\delta_1 + \delta_2}{2} \ldots \frac{\delta_{n-1} + \delta_n}{2}$, where the δ_i correspond to the measured points of the describing function, the following set of equations results:

$$\begin{cases} N\left(\frac{\delta_0 + \delta_1}{2}\right) = k_1 \\ N\left(\frac{\delta_1 + \delta_2}{2}\right) = (k_1 - k_2)S\left(\frac{2\delta_1}{\delta_1 + \delta_2}\right) + k_2 \\ N\left(\frac{\delta_2 + \delta_3}{2}\right) = (k_1 - k_2)S\left(\frac{2\delta_1}{\delta_2 + \delta_3}\right) + (k_2 - k_3)S\left(\frac{2\delta_2}{\delta_2 + \delta_3}\right) + k_3 \\ \cdots \\ N\left(\frac{\delta_{n-1} + \delta_n}{2}\right) = \sum_{i=1}^{n-1}(k_i - k_{i+1})S\left(\frac{2\delta_i}{\delta_{n-1} + \delta_n}\right) + k_n \\ \cdots \end{cases}$$

This equation system is trivially solvable by the substitution method. The so determined values will quantitatively represent the non linearity.

For the more general describing function forms the inversion is more complicated, but often possible.

It is intuitively clear that since the describing function is a simplified measure of nonlinear characteristic, the describing function inversion is necessarily non unique.

3.4 Further Considerations

Even if a large number of nonlinearities can be handled with the complex stiffness method, it is interesting to add some further considerations in order to reduce the restrictions imposed by the hypotheses:

1) Only the first (constant mass) imposed restriction is an actual limitation;

2) The fact that the stiffness has to be only dependent on the displacement is not necessary for the application of the method. It allows a simpler estimate of the mass value. As the damping is not important to the mass estimation, the previous consideration is even more valid for the first part of the third hypothesis. So significant conclusions can be drawn from the evolution of the equivalent parameter also if the first part of the second and third hypotheses is not satisfied **[3]**. In fact, by plotting the equivalent parameters as a function of both the displacement and the velocity, it is possible to know which parameters are a function of each other.

3) The restriction of the method to odd function of the displacement and the velocity is not absolutely an essential requirement for its application. It increases the easiness of understanding the results. In fact the describing function of a general nonlinear relationship contains both the real and the imaginary part. The direct principal consequence is that the k_{eq} and c_{eq} do not only correspond to the describing function of the stiffness and damping, but respectively to the describing function of the odd part of the stiffness plus the describing function of the even part of the damping and the describing function of the odd part of the damping plus the describing function of the even part of the stiffness; *i.e.* the describing function of the whole system has the form:

$$N^s(X) = \left[N_o^k - \omega^2 \overline{m} + \omega N_e^c\right] + j\left[\omega N_o^c + N_e^k\right]$$

In the case where the stiffness is a function of the only displacement, if a FRF obtained at constant displacement value is available, applying the complex stiffness method, both the real and the imaginary part of the stiffness describing function will result constant. The whole system describing function becomes:

$$N^s(X) = \left[\bar{k}_o - \omega^2 \overline{m} + \omega N_e^c\right] + j\left[\omega N_o^c + \bar{k}_e\right]$$

So it will be possible to verify whether the imaginary part of the describing function depends on an odd damping or on an even stiffness relationship. The same procedure can be applied if constant velocity FRFs are available.

4. RESULTS

The Complex Stiffness Method was applied to the lower frequency mode of all the FRFs shown in **Fig. 1**. They are the driving point responses at constant lateral force stepped sine excitation. The solid, dashed, dot-dashed, dotted lines indicate respectively the curve obtained at 150, 300, 525, 750 N force value.

Before introducing the results, it is important to point out the following aspects:

1) The values obtained directly by the complex stiffness method application, are not the actual nonlinear characteristics, but their point by point linearisation according to the describing function procedure. They give only qualitative information about the behaviour of the investigated parameter;

2) The displacement and the velocity, which are being dealt with, are the values obtained by the FRFs curves, that is the lateral displacement and velocity of the helicopter mast.

4.1 Equivalent Mass

The first step of the method is the mass calculation. In **Fig. 2** the mass estimated values, obtained in the range of interest for each spectral line, are depicted as functions of the displacement.

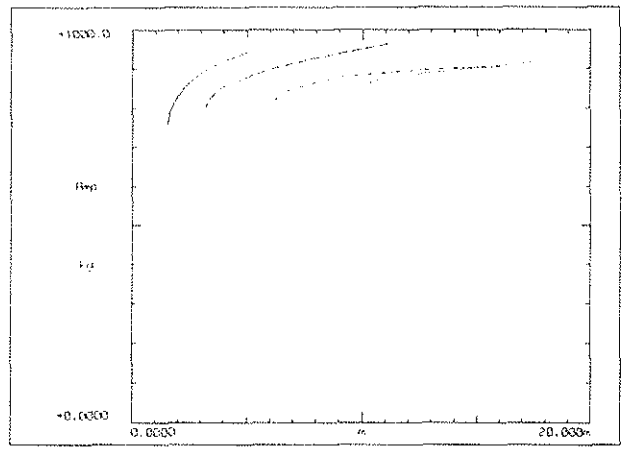

Fig. 2 - Mass estimates as a function of displacement.

It is possible to see that the equivalent mass is not constant but it increases approaching the resonance.

In order to overcome this effect, also the alternative method was applied to three frequencies values (1.33, 1.45, 1.6 *Hz*) well far from the resonance peaks.

The values obtained by using both the method are listed in the following tables.

Force [N]	150	300	525	750	Mean Value
Mass [kg]	826.4	862.3	863.2	872.3	856.0

Tab. 1 - Average mass values estimated at different excitation force levels together their global average.

Frequency [Hz]]	1.33	1.45	1.6	Mean Value
Mass [kg]	819.8.	829.9	891.2	846.9

Tab. 2 - Mass values estimated at constant frequencies excitation and their average.

It is important to note that the assessed mass is not the actual mass of the whole helicopter but the modal mass, *i.e.* the mass involved in the considered mode.

The estimates of the values, obtained for the different force levels, are quite consistent. Furthermore there is a very good agreement between the results of the two methods.

4.2 Equivalent Stiffness

Next the equivalent stiffnesses were obtained for the four FRFs. They are displayed in **Fig. 3** against the displacement.

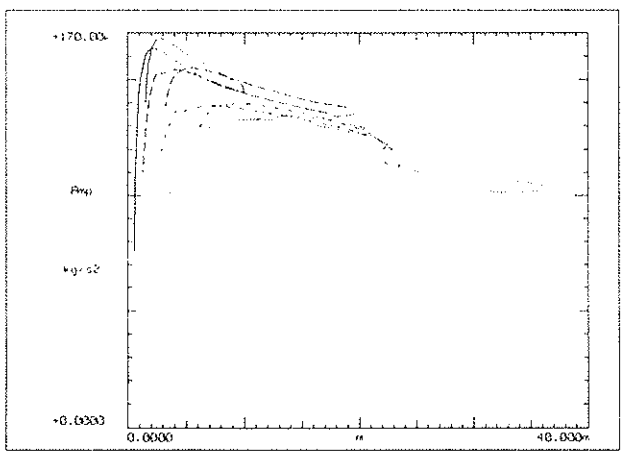

Fig. 3 - Equivalent stiffness (or real part of the system describing function) as function of the displacement.

Just at a first view the results are quite consistent. It is also clear that, as it was easily predicted, the equivalent stiffness indicates a softening stiffness nonlinearity.

From a more particular point of view it is possible to define three typical trends:

1) From 0 to about few millimetres, the equivalent stiffness increases from a very small value to a maximum;

2) Then it begins to regularly decrease as displacement increases up to about 22 *mm*;

3) Finally after a sharp drop to a lower level, it continues to decrease to a constant value.

A stiffness trend equal to the first is representative of the presence of free-plays. To exclude the effects of the interface between the helicopter and the shaker, different kinds of links were used. No significant differences were found. So such behaviour is attributable to free-plays present in the main gearbox or/and in the landing gear system.

In the second the effects of a softening nonlinearity, distributed or concentrated somewhere in the helicopter, could be recognized. Such a behaviour is typical of the landing-gear shock absorber plus pneumatic tire system.

Then the sudden drop could depend on the modification of the stiffness when the rod of the landing gear shock absorber starts to move (indeed this was visible near the resonance only at high excitation force level, that is for high displacement values).

4.3 Equivalent Damping

The equivalent damping were obtained. In **Fig. 4** the extracted functions are depicted versus the velocity.

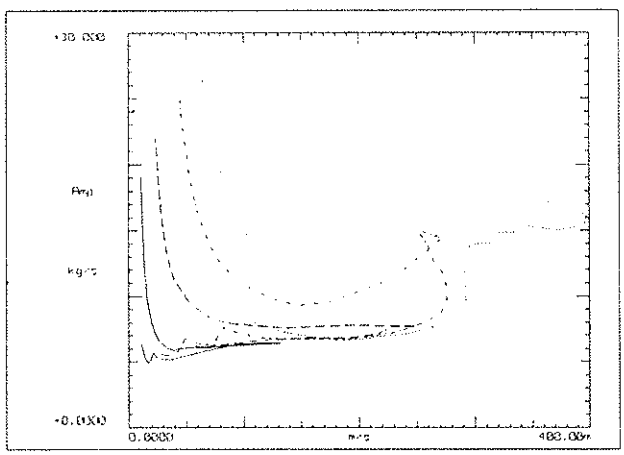

Fig. 4 - Equivalent damping (or imaginary part of the system describing function) as function of the velocity.

It is possible to divide the evolution of the damping in four different characteristic section:

1) A very rapid decrease from a very high value;

2) Then sudden increase and decrease of the damping are visible for a displacement value comprised between 2 and 15 mm. This

behaviour is only visible in the branch obtained for decreasing velocity;

3) A quite constant value;

4) Finally a sharp increase up to a maximum where it remains constant (This behaviour is visible only for the high force level curve, that is for high velocity).

These different behaviours suggest the following considerations:

The physical meaning of the behaviour in the first range is not clear. In the following, by reducing the simplifying hypotheses, a possible interpretation will be given.

The peaks due to increasing and decreasing is a characteristic of friction damping. The fact that the displacement is not large excludes its belonging to the landing gear dampers. It could be probably connected to the recovering of some freeplays or to the wobbling pneumatic tires.

The large increasing coincides with the starting of the motion of the damping struts of the landing gear dampers. It could be the effect of the friction in the shock dampers. In this case a further increasing in the velocity could give a reduction of the values.

4.4 Further considerations

As it is possible to see in the previous figures, the equivalent curves have two branches: one obtained for increasing displacement and the other for decreasing displacement. According to theory they have to be identical. The differences occurring are attributable to one of the following facts:

1) As the resolution of the curves becomes poor, approaching the natural frequency, it is difficult to avoid discontinuities or jumps at the high values of the displacement and velocity;

2) Small phase shifts, due to filters and amplifiers of the sensor, occurred during the acquisition can produce relatively large differences between the FRF values below and above the resonance. This causes deviations between the two branches of the curves particularly at low frequency;

3) The equivalent characteristic depends on the other parameter; (stiffness on velocity and damping on displacement). A check of the remaining possibility was performed. In the following figures (**Figs. 5** and 6) the equivalent stiffness is plotted against the velocity and the damping versus the displacement. Comparing them with **Figs 3** and **4**, no significant differences are visible. Indeed, as the analysis range falls between low frequency values, no large modifications are obtainable by the passage from displacement to velocity and viceversa.

4) The parameter is also function of the frequency.

5) The investigated parameter is not a purely odd function of displacement or velocity.

This suggests an intriguing explanation of the unjustifiable behaviour visible in the describing function of the damping: it is attributable to the existence of an even part of the stiffness. Indeed, as it had just been said, the not odd part of the stiffness appears in the equivalent damping. Furthermore its trend is quite similar to the imaginary part of the describing function of backlash nonlinearity (see **Appendix A2** for more detail on this nonlinearity). To verify this interesting hypothesis the complex stiffness method was applied at a set of FRFs obtained with constant displacement. The unjustifiable trend of the damping disappeared. As, in the hypothesis of a stiffness depending only on the displacement, it is reliable to consider its effects negligible both in the real and the imaginary part of the describing function, it is possible to assume such trend as the effect of the not odd part of the stiffness relationship.

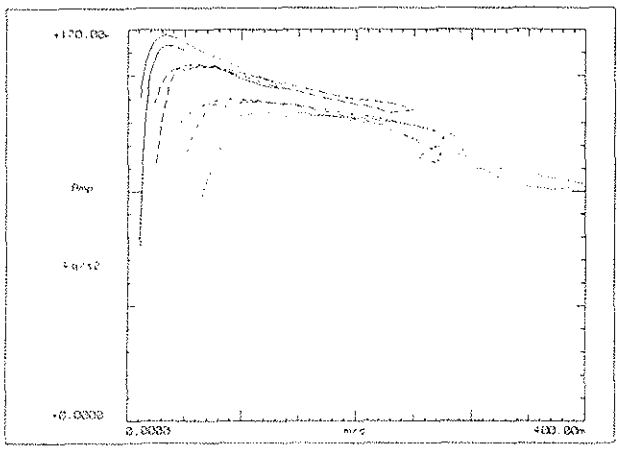

Fig. 5 - Equivalent damping redrawn as function of the velocity.

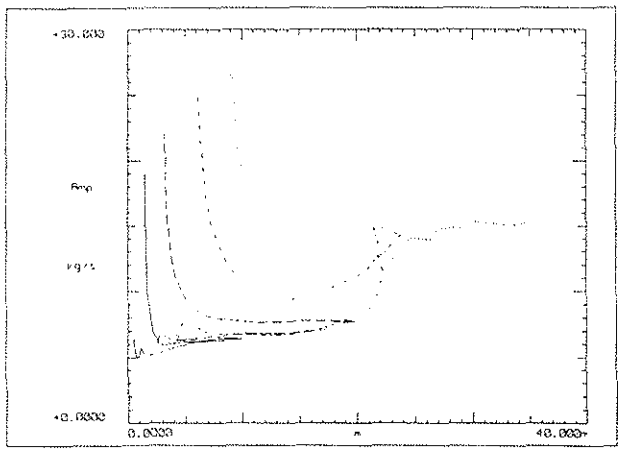

Fig. 6 - Equivalent damping redrawn as function of the displacement.

The result suggests that the assumption could be true and confirms that also not odd characteristics can be treated with the complex stiffness method.

If constant velocity FRFs had been acquired the *same procedure can be repeated, in case it is* necessary, on the equivalent stiffness, giving information on the imaginary part of the damping describing function.

5. ACTUAL VALUES OF THE PARAMETERS

The actual values of the characteristics were obtained by inverting the describing function by using the outlined method. In the following **Figs. 7-8** the actual nonlinear stiffness is depicted versus the displacement. The inversion operation increases the differences between the values obtained for increasing (**Fig. 7**) and decreasing **(Fig. 8)** displacement values.

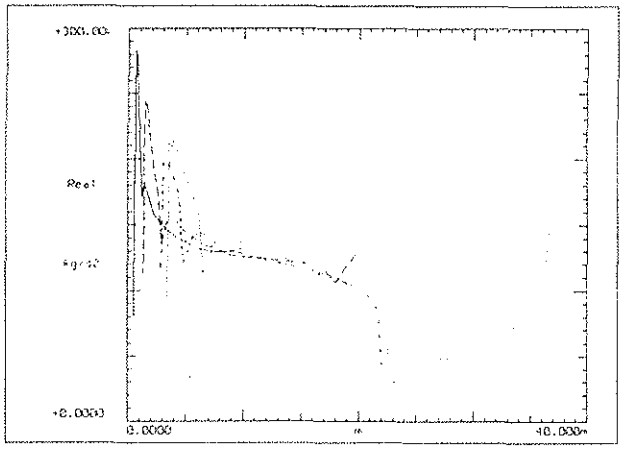

Fig. 7 - Original nonlinear stiffness (or inverted real part of the describing function) obtained for increasing displacement plotted as function of the displacement. .

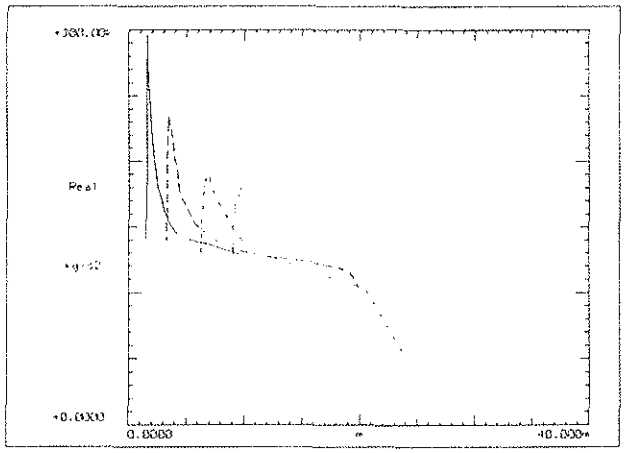

Fig. 8 - Original nonlinear stiffness obtained for decreasing displacement shown as function of the displacement.

In the following the actual nonlinear damping relationships obtained from both the increasing (**Fig 9**) and the decreasing (**Fig 10**) velocity branches of its describing function are shown.

Again the differences between the two cases are amplified by the describing function inversion. In particular the high negative slope deforms the initial trend of the first figure, introducing meaningless negative values.

It is important to note the dependence on the *frequency of the damping, recognizable in the shift of* the peaks occurring in **Fig. 10**. This is a characteristic trend of the friction damping.

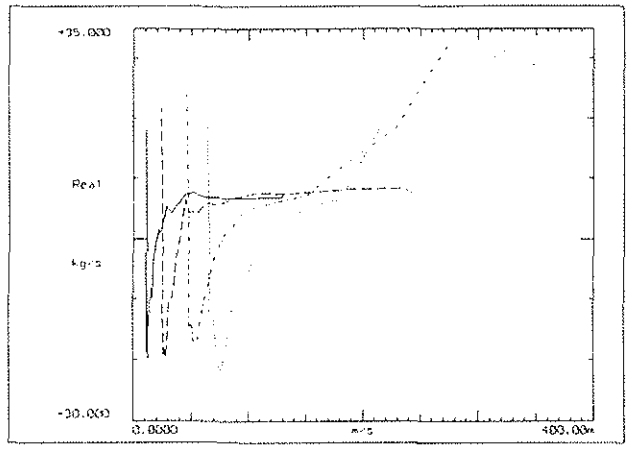

Fig. 9 - Original nonlinear damping (or inverted imaginary part of the system describing function) obtained for increasing velocity values shown as function of the velocity.

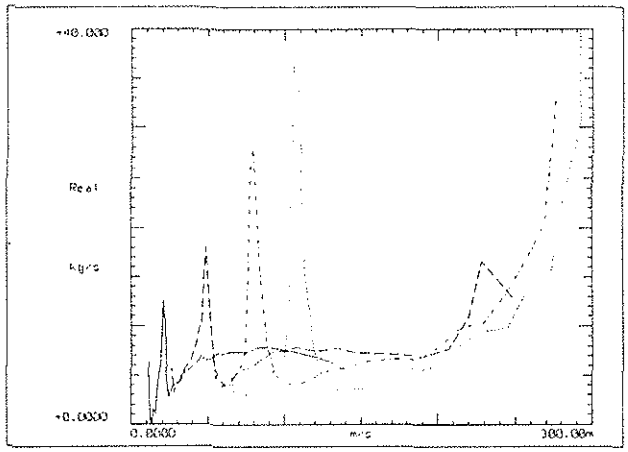

Fig. 10 - Original nonlinear damping obtained for decreasing velocity values depicted as function of the velocity.

6. CONCLUSIONS

The intent of the study was to provide information leading from a *experimentally obtained FRF*

to a better understanding of a nonlinear system behaviour and an identification of the nonlinear parameters. Even though the used technique is only applicable to SDOF systems it was possible to detect the trends of the nonlinear stiffness and damping present in the investigated helicopter airframe.

Moreover the possibility of extending this method to handle also non-odd nonlinear characteristics, commonly found in real structures, prospects future practical applications.

7. ACKNOWLEDGMENT

The authors wish thank Mr Fausto Cenedese for his precious contribution during the experimental phase of the activity and Mr Maurizio Parodi from LMS Italiana.

8.REFERENCES

1 - J. He and D.J. Ewins, *A simple Method of interpretation for the modal analysis of nonlinear systems*, Proceedings of the 5th International Modal Analysis Conference, April 1987.

2 - K. Wyckaert, P. Vanmerck, P. Sas, H. Van Brussel, *The identification of the nonlinear dynamical behaviour of a flexible robot link*, Proceedings of the 15th Internal seminar On Modal Analysis, Sept. 1990.

3 - P.Vanmerck, H.Van Brussel, M. Mertens , K. Wyckaert, *Parametric identification of non-linear systems*, Proceedings of the 13th Internal Seminar On Modal Analysis, Sept. 1988.

4 - H. Van der Auweraer, K. Wyckaert, *Experimental Analysis of nonlinear Behaviour of an aerospace structure*, Proceedings of Florence Modal Analysis Conference, Sept. 1991.

5 - J.B. Truxal, Control system synthesis., Mc Graw-Hill International Edition. 1955.

6 - Bernard Friedland, Control system design., Mc Graw-Hill International Edition. 1987.

7 - E.J. Slotine, W. Li, Applied nonlinear control., Prentice-Hall 1991.

8 - I.J. Nagrath, M. Gopal, Control system engineering., John Wiley & Son 1987.

9 - M.Mertens, P. Vannerck, H.Van der Auweraer, R. Snoeys, *Measuring and evaluating nonlinear dynamic behaviour of mechanical structures using sinusoidal excitation*, Proceedings of the 5th International Modal Analysis Conference, April 1987.

A. APPENDICES

A.1 Describing Function of a Simple Odd Piecewise Linear Nonlinearity

In the following (**Fig. A1.1**) the input/output relationship of a nonlinear system characterized by a dead-zone plus a saturation is depicted. Where X_0 and X_s are respectively the ranges of the dead-zone and the saturation, k denotes the slope of the nonlinearity.

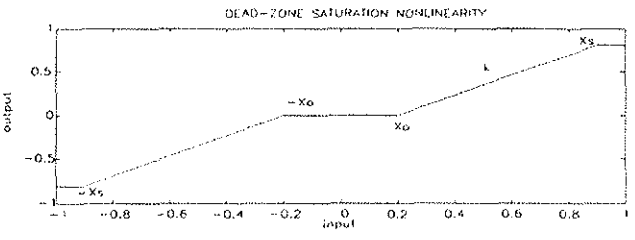

Fig. A1.1 - Output/input relation for a dead-zone and saturation nonlinearity.

Now consider the pure sinusoidal input $Ysin(\omega t)$; if $Y > X_s$, the output will be expressed, in a half cycle, as:

$$w(t)\begin{cases} 0 & 0 \le \omega t \le \alpha \\ k(Ysin(\omega t) - X_0) & \alpha \le \omega t \le \beta \\ k(X_s - X_0) & \beta \le \omega t \le (\pi - \beta) \\ k(Ysin(\omega t) - X_0) & (\pi - \beta) \le \omega t \le (\pi - \alpha) \\ 0 & (\pi - \alpha) \le \omega t \le \pi \end{cases}$$

where $\alpha = sin^{-1}\left(\frac{X_0}{Y}\right)$ and $\beta = sin^{-1}\left(\frac{X_s}{Y}\right)$.

The input and the output are plotted in **Fig. A1.2**.

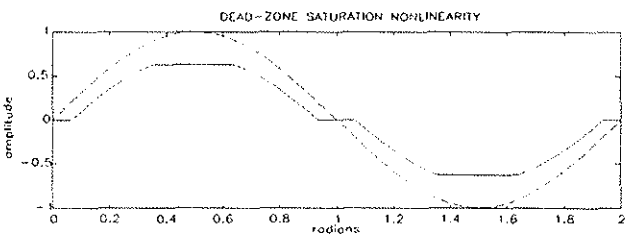

Fig. A1.2 - Output and input wave for a dead-zone and saturation nonlinearity.

The odd nature of $w(t)$ implies that $A_1 = 0$ and the symmetry over the four quarts of a period brings that:

$$B_1 = \frac{4}{\pi}\int_0^{\frac{\pi}{2}} w(t)sin(\omega t)d(\omega t) =$$

$$= \frac{4}{\pi}\left\{\int_\alpha^\beta k[Ysin(\omega t) - X_0]d(\omega t) + \int_\gamma^{\frac{\pi}{2}} k(X_s - X_0)sin(\omega t)d(\omega t)\right\}$$

According to its definition the describing function is:

$$N(Y) = \frac{B_1}{Y} = \begin{cases} 0 & 0 \le Y \le X_0 \\ 1 - \frac{2k}{\pi}[\alpha + sin\alpha cos\alpha] & X_0 < Y \le X_s \\ \frac{k}{\pi}[2(\beta - \alpha) + (sin2\beta - sin2\alpha)] & Y > X_s \end{cases}$$

The describing function is plotted in **Fig. A1.3** as a function of Y/X_S.

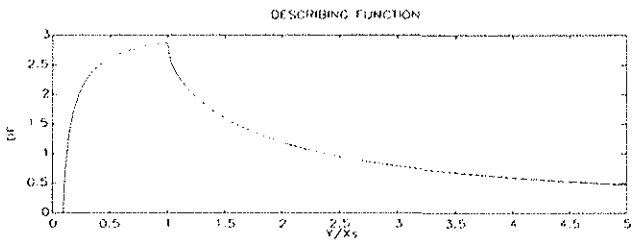

Fig. A1.3 - Describing function of the dead-zone and saturation nonlinearity.

The output is null since the input is lower than the dead-zone range. Then, as it is intuitively reasonable the $N(Y)$ firstly increases, because the effects of the dead-zone gradually diminishes as the amplitude of the input increases up to X_s, then decreases, since the saturation amounts reduces its ratio to the output.

On the other hand by use of the general expression given in the **par 3.3**, with $n = 2$, X_0 and X_s being the two breakpoints, and k as the slope, the following expression will be obtained.

$$N(Y) = k\left[1 - S\left(\frac{X_0}{Y}\right)\right] + S\left(\frac{X_S}{Y}\right)$$

It is possible to show, with simple manipulations, that such expression is identical to the previous.

A.2 Describing Function of the Backlash Nonlinearity.

Fig. A2.1 shows the output/input relationship of a backlash nonlinearity, with slope k and width $2X_0$. If the input amplitude is smaller than X_0, there will be no output.

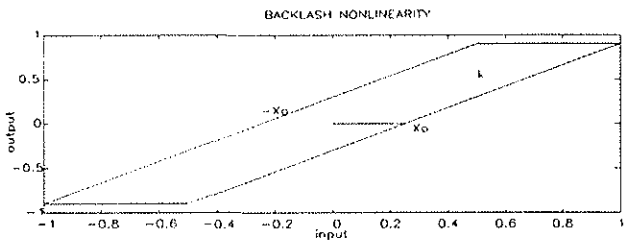

Fig. A2.1 - Output/input relation for a backlash nonlinearity.

If the input is $Ysin(\omega t)$.the output wave $w(t)$ can be described, in a period, as follows:

$$w(t) = \begin{cases} (X - b)k & \frac{\pi}{2} \le \omega t \le \pi - \gamma \\ (Xsin(\omega t) + b)k & \pi - \gamma \le \omega t \le \frac{3\pi}{2} \\ -(X - b)k & \frac{3\pi}{2} \le \omega t \le 2\pi - \gamma \\ (Xsin(\omega t) - b)k & 2\pi - \gamma \le \omega t \le \frac{5\pi}{2} \end{cases}$$

where $\gamma = sin^{-1}\left(1 - \frac{2b}{X}\right)$

The output $w(t)$ of the nonlinearity is as shown in the **Fig. A2.2**.

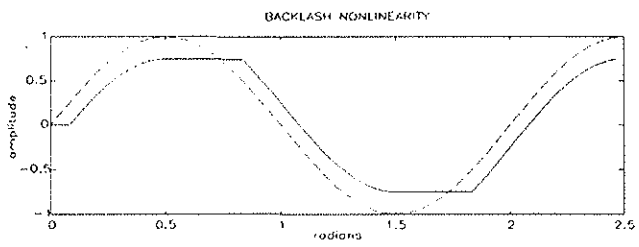

Fig. A2.2 - Output and input wave for a backlash nonlinearity.

The function $w(t)$ is neither odd nor even. Therefore, both A_1 and B_1 are non-zero. Through some tedious but not difficult integrations the following expressions are obtained:

$$A_1 = \frac{4kX_0}{\pi}\left(\frac{X_0}{Y} - 1\right)$$

$$B_1 = \frac{Ak}{\pi}\left[\frac{\pi}{2} - \sin^{-1}\left(\frac{2X_0}{Y} - 1\right) - \left(\frac{2X_0}{Y} - 1\right)\sqrt{1 - \left(\frac{2X_0}{Y} - 1\right)^2}\right]$$

The real or the imaginary parts of the describing function are (or the describing functions respectively of the odd and even parts of the input/output relationship) plotted in **Fig. A2.3**.

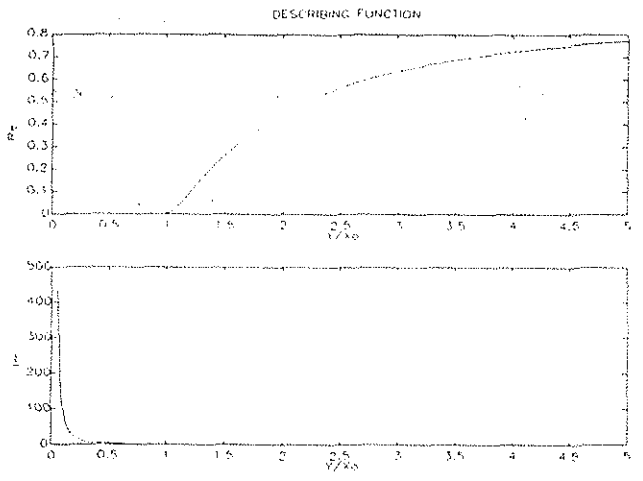

Fig. A2.3 - Real and imaginary part of the backlash describing function.

Note that the presence of a non-zero imaginary part brings a phase lag. This lag is the reflection of the gap that introduces a time delay.